Development of frequency converter for high-power laser facility

Keyu Li (李恪宇), Fuquan Li (李富全), Bin Feng (冯 斌), Huaiting Jia (贾怀庭), Yong Xiang (向 勇), Wei Zhong (钟 伟), Fang Wang (王 芳), Bing Xu (徐 冰), Tian'en Li (李天恩), Liquan Wang (王礼权), Chunzhuo Zhao (赵春卓), Chi Ma (马 弛), Feng Jing (景 峰), and Xiaofeng Wei (魏晓峰)

Research Center of Laser Fusion, China Academy of Engineering Physics, Mianyang 621900

The Technical Integration Experiment Line (TIL) prototype for Shenguang (SG) III laser facility at Research Center of Laser Fusion (RCLF) of China Academy of Engineering Physics (CAEP) has commissioned the first beam line into the diagnostic target chamber. The facility has demonstrated frequency converted Nd:glass laser energies from a single beamline of 1.43 kJ for 1.3-ns nearly flat-top pulse and 2.75 kJ for 3-ns flat-top one at 3ω in 2006, namely third harmonic generation (THG) efficiency of 65%−70% for two states. This paper describes comprehensive and precise theory and experiment analysis of frequency converter development and factors affecting THG efficiency for high-power laser facility.

OCIS codes: 190.2620, 120.4820.

For large inertial confinement fusion (ICF) laser facilities all over the world, it is the magnificent goal for all scientists to gain stable and high-efficiency third harmonic generation (THG). The 3ω energy output ability of Technical Integration Experiment Line (TIL) is the most key technique and also one of bottlenecks affecting the laser operation. Therefore, the main theory, techniques and project problems about THG system have been studied for TIL prototype facility, and varieties of factors that influence THG efficiency for large-aperture, high-fluence THG in ICF laser have been analyzed in detail. To increase the THG efficiency, the homologous control means have been adopted and the anticipant result has been implemented. Although there are many published papers on THG[1−3], in this paper the THG physical process and the actors affecting THG efficiency are studied and analyzed specially by theoretical simulations and experiment data of large ICF laser facilities. The experiment results will provide experiment proofs and calculation tools for eight beam eligibility and power balance of TIL prototype laser facility.

Figure 1 shows the development of frequency converter for main high-power laser facilities of the world. The external THG efficiency exaltation of 15% for TIL has come true in the past three years, and the next goal is to make the external THG efficiency be up to 70%−75% in 2007.

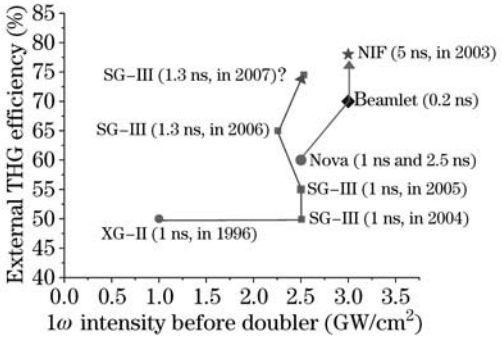

Fig. 1. Frequency converter development for main high-power laser facilities.

The TIL facility is designed as an 8 laser beam target irradiation facility to perform ICF and high energy density experiments, as shown in Fig. 2. Figure 3 shows the type I final optical assembly (FOA) and THG system in the experiment. The design of THG system incorporates a type I/type II third harmonic generator to convert the 1.053 μm fundamental wavelength of the laser amplifier to a wavelength of 0.351 μm for target irradiation, as indicated in Fig. 4.

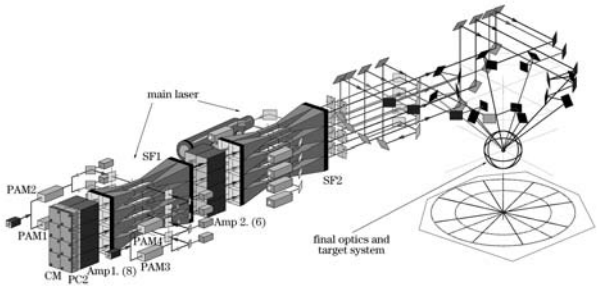

Fig. 2. TIL laser facility beam layout.

Fig. 3. FOA and THG system in the experiment.

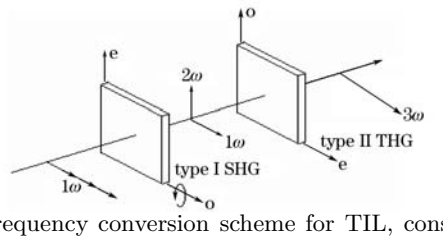

Fig. 4. Frequency conversion scheme for TIL, consisting of a 11.8-mm type-I KDP doubler and a 9-mm type-II KDP tripler.

Based on Maxwell equations and wave theory, and considering the following physical processes and parameters: 1) two-order nonlinear three-wave mixing (doubling and tripling), 2) crystal absorption and reflection from crystal surfaces, 3) bulk linear loss, 4) diffraction, 5) Poynting vector walk-off, 6) nonlinear refractive index, and with the following definitions for the three fields ($l = 1, 2, 3$):

$$E_l(x, y, z, t) = \frac{1}{2}\frac{1}{\sqrt{n_l}} A_l(x, y, z, t) \exp(ik_l z - \omega_l t) + c.c., \tag{1}$$

the coupling equation for the sum-generated field A_{3e} has the form of[1−6]

$$\begin{aligned}
&\frac{\partial A_{3e}}{\partial z} + \frac{1}{v_3}\frac{\partial A_{3e}}{\partial t} = \frac{i}{2k_3}\nabla^2 A_{3e} - \rho_3 \frac{\partial A_{3e}}{\partial y} \\
&+\frac{i3\omega}{2n_3 c}\overline{\chi} A_{1e} A_{2o} e^{-i\Delta k z} - \frac{1}{2}\alpha_3 A_{3e} \\
&+\frac{i3\varepsilon_0 n_3 \omega}{2}[2\gamma_{31}|A_{1e}|^2 + 2\gamma_{32}|A_{2o}|^2 + \gamma_{33}|A_{3e}|^2]A_{3e},
\end{aligned} \tag{2}$$

with similar equations applying for 1ω field A_1 and 2ω field A_2. The first and the second terms at the left of Eq. (2) show respectively the changes of field amplitudes along the z direction of propagation and time t. The five terms on the right describe in turn diffraction, walk-off, crystal absorption and reflection, nonlinear conversion, and nonlinear loss.

According to coupling equations, the approximate solution to THG efficiency in small signal is

$$\eta_{\mathrm{THG}} = \kappa \times I_{1\omega} \times \sin c^2(\Delta k \times L/2). \tag{3}$$

The above solution indicates that η_{THG} is the function of $I_{1\omega}$, Δk (phase-mismatch value) and the crystal thickness L. In the above expression, the quantity has by far the greatest impact on THG efficiency, and it is also the most sensitive to operating conditions, caused by the momentum mismatch between the three fields:

$$\begin{aligned}
\Delta k &= k_{A_{3e}} - k_{A_{2o}} - k_{A_{1e}} \\
&= (1/c) \times (\omega_3^{e}(\theta)\, n_3^{e}(\theta) - \omega_2^{o} n_2^{o} - \omega_1^{e}(\theta)\, n_1^{e}(\theta)),
\end{aligned} \tag{4}$$

which depends critically on the material birefringence (refractive indices n_l), and thus on the frequency of the input fields ω_2^{o}, ω_1^{e}, the crystal temperature T, and the orientation θ of the crystal optic axis with respect to the field propagation direction.

$I_{1\omega}(x, y, t)$ is the three-dimensional (3D) function of space and time[7], that is to say, $I_{1\omega}$ bears on the near field distribution and pulse shape. If they tend to be square, THG efficiency will be high. Whereas, different degrees of disturbance and modulation of $I_{1\omega}(x, y, t)$ will lead badly to the decrease of THG efficiency. By using the following data numbered 20041215001 (a typical set of parameters, it means the first laser shot data on Dec. 15, 2004): the average $I_{1\omega}$ of 2.6 GW/cm^2, a similar flat-top 1ω intensity distribution and the 1ω modulation degree (the ratio of peak irradiance to average irradiance) M of 1.57, the contrast (the ratio of sigma to average irradiance) C of 0.12, the influences of near field distribution and pulse shape on efficiency are obtained, as shown in Figs. 5 and 6.

From the figures, it can be seen that the influence of pulse shape on efficiency is more than that of the near field distribution. The near field modulation leads to a little reduction of about 1% in THG efficiency or so. The Gaussian pulse results in a decrease of about 9% of THG efficiency, and the flat pulse leads to higher THG efficiency than Gaussian pulse. It can also be seen that the near field modulation has little effect on THG efficiency when TIL runs on the stage of the average $I_{1\omega}$ of 2.6 GW/cm^2.

But the pulse modulation has more effect on THG efficiency. From Fig. 5(d) and Fig. 6, it is shown that $I_{1\omega}(t)$ at different duration time is equal basically for square pulse, so the THG efficiency is also coincident in the whole duration time and the high-efficiency THG will be gained. Whereas there is too long foot pulse in the rising and falling widths for Gaussian and triangle pulses, where $I_{1\omega}(t)$ is lower than that during the flat

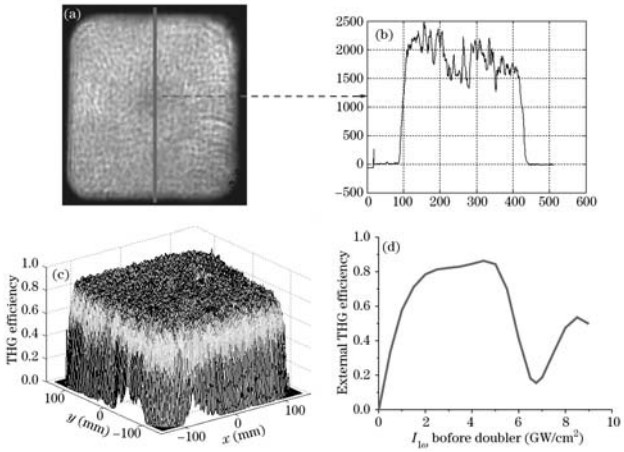

Fig. 5. Influence of near field distribution on THG efficiency in ideal square pulse. (a) Measured two-dimensional (2D) 1ω near field; (b) measured one-dimensional (1D) 1ω near field distribution; (c) calculated THG efficiency distribution versus space; (d) calculated external THG efficiency versus input 1ω irradiance under the optimized crystal thickness for TIL prototype laser facility.

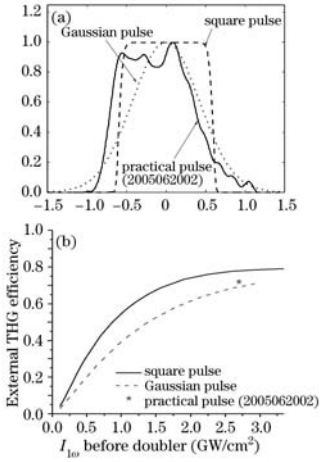

Fig. 6. Influences of three pulse shapes on efficiency in ideal square 1ω near field distribution. (a) Three pulse shapes; (b) calculated THG efficiency versus 1ω irradiance.

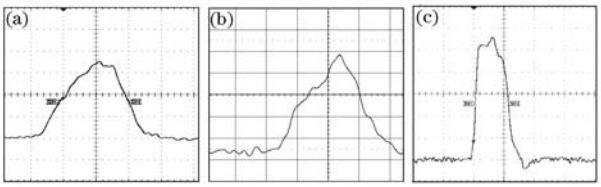

Fig. 7. Three typical pulse shapes in the past three years for (a) triangle pulse in 2004, (b) triangle pulse in 2005, and (c) nearly square pulse in 2006.

area out and away, so does the efficiency. As a result, the average efficiency in the duration pulse lowers consumedly. As shown in Fig. 7, pulse shape tends similar flat step by step in 2006, which contributes to THG efficiency exaltation partially in the past three years.

$\Delta k(x, y)$ is a space 2D function. The non-uniformity of Δk at different area in near field will lead to spatial variations in efficiency. And $\Delta k(x, y)$ is also the function of tuned-angle $\beta(x, y)$, so $\beta(x, y)$ should be controlled in the experiments. In high-intensity THG the mixing ratio of photons between 2ω and 1ω is required to be 1:1 before tripler to realize high-efficiency THG, which is accomplished by angular detuning of the doubler in the type I/type II tuned-angle design. So the whole system especially the doubler is very sensitive to angular errors, and $\Delta k(x, y)$ is caused by the following three factors.

Firstly, the influence of tuned-angle β's error $\Delta\beta$. In Figs. 8 and 9, it is shown that owing to error of the crystal cut angle, when the THG efficiency is the highest, the laser transmits to the crystal surface in the means of oblique incidence instead of normal incidence, and the angle of incidence is crystal optimal matched angle θ. For example, in the experiment θ of doubler and tripler are -27.245 and 1.860 mrad in turn. Based on optimal match of the two crystals, the doubler will be tuned at a certain angle named designed tuned-angle $\beta_{\rm d}$ to realize 1:1 mixing ratio of photons between 2ω and 1ω along with the rise of $I_{1\omega}$, but the tripler is matched for ever, namely $\beta_{\rm d}$ of 0. Whereas, there is an error $\Delta\beta$ between designed and practical tuned-angle β owing to many factors. In 2006, by using 1ω crystal alignment laser system shown in Fig. 10, the error $\Delta\beta$ has been controlled and reduced consumedly, which contributes to THG efficiency exaltation primarily in 2006 partially.

Secondly, the influence of wavefront radius R. The contour of wavefront is a spherical surface with the radius R, which is the wavefront aberration at low frequency. It is induced by the 1ω wavefront radius and the aberrations of surface figure of crystals.

Thirdly, the influence of crystal refractive indices uniformity. Figure 11(a) shows the histograms of representative Δn distributions obtained from orthogonal-polarization interferograms of crystals used in 2004 and 2006, expressed in terms of equivalent detuning angles, and the crystals quality in 2006 is better than that in 2004 out and away. The equivalent detuning angles were calculated by assigning the variations in Δn to local changes in the direction of the crystal optic axis. The relative impacts of these angular distributions on 3ω conversion efficiency have been calculated separately using the plane wave model, and are plotted versus drive irradiance in Figs. 11(b) and (c). The very good crystal quality in 2006 contributes to the THG efficiency exaltation primarily.

Fourthly, the influence of wavefront modulation. Besides error $\Delta\beta$, wavefront radius and crystal quality, there are middle and high frequency modulations at the contour of wavefront which are caused by the following four factors: dust at air path, modulations of 1ω wavefront caused by nonlinear effect, small-scale periodicity traces at the crystals surface caused by machining, defects inside and outside the crystals. The later two factors can be indicated by measuring the transmission wavefront of crystals, and the influence of wavefront modulation caused by crystal machining is up to 1% or so, but crystal wavefront modulation will have much effect on the modulation degree of 3ω near field.

In the above four factors affecting mismatch Δk, the pivotal ones are crystal refractive indices, tuned-angle error $\Delta\beta$, wavefront radius R, and wavefront modulation in turn.

Now let us consider the influence of the crystal thickness L on the THG efficiency. As shown in Fig. 12 and Fig. 5(d), the two crystal thicknesses have been optimized under ideal condition to ensure high-efficiency THG for TIL, and the optimized result consists of a 11.8-mm type-I KDP doubler and a 9-mm type-II KDP tripler. When TIL works at designed optimized condition, namely $I_{1\omega}$ of 2.7−3 GW/cm^2 for 1 ns in square

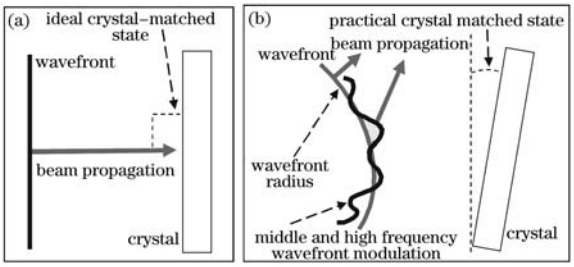

Fig. 8. Mismatch Δk under (a) ideal ($\Delta k = 0$) and (b) practical ($\Delta k \neq 0$) conditions.

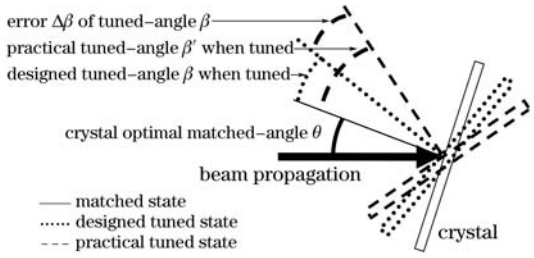

Fig. 9. Matched, designed, and practical crystal states.

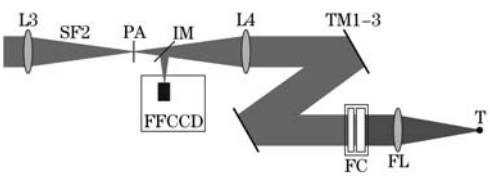

Fig. 10. 3ω target alignment and 1ω crystal alignment laser system. PA: pinhole; FC: crystal; FL: focusing lens; T: target; SF2: spatial filter; L: lens; TM: transmission mirror.

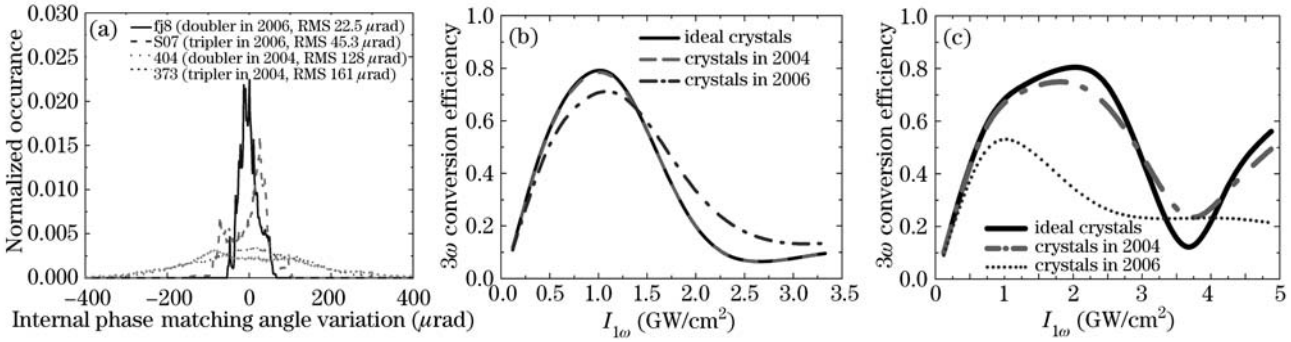

Fig. 11. (a) Distribution of phase-match angles in the crystals inferred from orthogonal-polarization interferometry; (b) and (c) plane-wave calculation showing the effect of individual distributions on 3ω conversion efficiency versus 1ω irradiance with the nominal detuning angles for the doublers of 0 and 220 μrad in turn.

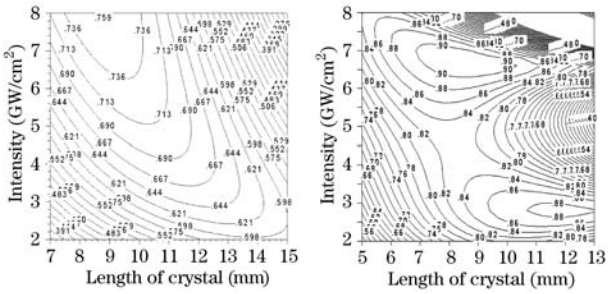

Fig. 12. Thickness optimization of the two crystals under ideal condition. (a) The contour of the internal SHG efficiency as a function of $I_{1\omega}$ and the doubler thickness; (b) the contour of the external THG efficiency as a function of $I_{1\omega}$ and the tripler thickness.

pulse shape and square near field, the internal SHG efficiency is 67% or so and external THG efficiency is up to 80% as Fig. 5(d) shows. That is to say, the optimized thickness of the crystals has met the demand of TIL.

The important factors affecting THG efficiency are refractive indices uniformity, time modulation, and error $\Delta\beta$. And THG efficiency exaltation of 15% for TIL owes to good crystal with refractive indices uniformity, similar flat-topped pulse and lower error $\Delta\beta$.

In conclusion, by analyzing the three factors affecting THG efficiency, external THG efficiency exaltation of 15% and the reason why the measured maximum value of THG efficiency is up to 65%−70% in experiment have been made clearly, and the development of frequency converter for TIL owes to good crystal with refractive indices uniformity, similar flat-topped pulse and lower error $\Delta\beta$. The coherence between experiment and simulation calculation has been proved. Furthermore, the correlative data have been gained to implement eight beam eligibility and the power balance in the year of 2007. And the work emphases in the future include keeping a very good crystal quality, shaping the 1ω pulse to be square, improving the surface figure quality of crystals, improving the beam alignment technique and the measure precision of crystal optimal matched-angle, improving beam path lustration and controlling the middle and high frequency modulations at the surface of optical elements. The THG efficiency for TIL prototype laser facility will be up to 70%−75% in the future.

This work was supported by the National 863-804 Project of China. The authors also wish to thank for Academician Dianyuan Fan, Xiaomin Zhang, Wanguo Zheng, Zhang Shui, Dongxia Hu, Bo Chen, Jingqin Su, and Chengcheng Wang *et al.* for their helps in the experiment and fruitful discussions. K. Li's e-mail address is likeyu6969@56.com.

References

1. J. A. Armstrong, Phys. Rev. **127,** 1918 (1962).
2. R. S. Craxton, IEEE J. Quantum Electron. **17,** 1771 (1981).
3. P. W. Milonni, J. M. Auerbach, and D. Eimerl, Proc. SPIE **2622,** 230 (1997).
4. P. J. Wegner, J. M. Auerbach, C. E. Barker, S. C. Burkhart, S. A. Couture, J. J. DeYoreo R. L. Hibbard, L. W. Liou, M. A. Norton, P. K. Whitman, and L. A. Hackel, Proc. SPIE **3492,** 392 (1999).
5. Y. Wang, B. Luther-Davies, Y.-H. Chuang, R. S. Craxton, and D. D. Meyerhofer, Opt. Lett. **16,** 1862 (1991).
6. M. Auerbach, C. E. Barker, D. Eimerl, K. R. Manes, D. Milan, P. W. Milonni, J. B. Trenholme, B. Van Wonterghem, "Frequency conversion modeling" UCRL-LR-105821-96-4 (1996) p.199.
7. P. W. Milonni, J. M. Auerbach, and D. Eimerl, Proc. SPIE **2633,** 494 (1997).